Doc Ophthalmol (2007) 115:203–209
DOI 10.1007/s10633-007-9077-6

ORIGINAL RESEARCH ARTICLE

# Functional study in NSE-Hu-Bcl-2 transgenic mice: a model for retinal diseases starting in Müller cells

**Cécile Péant · André Dosso · Lorenza Eder-Colli · Florence Chiodini**

Received: 15 March 2007 / Accepted: 23 July 2007 / Published online: 7 August 2007


**Abstract** In NSE-Hu-Bcl-2 transgenic mice, line 71, retina undergoes early postnatal degeneration linked to the prior death of Müller cells. The purpose of this study was to complete the characterization of this retinal dysfunction by using electroretinographic (ERG) recordings in both scotopic and photopic conditions. Here, we showed that both rod and cone systems were profoundly affected in NSE-Hu-Bcl-2 transgenic mice as soon as 15 postnatal days in accordance with histological study performed previously.

**Keywords** Bcl-2 over-expression · Electroretinogram · Müller cells · Photoreceptors · Retinal degeneration

**Abbreviations**

| | |
|---|---|
| cds/m$^2$ | Candelas*second/m$^2$ |
| ERG | Electroretinography |
| IT | Implicit time |
| MCs | Müller glial cells |
| NSE-Hu-Bcl-2 mouse | Mouse over-expressing the human Bcl-2 under the control of neuron-specific enolase promotor |
| OPs | Oscillatory potentials |
| PN | Postnatal day |
| WT | Wild-type |
| tg | Transgenic |

C. Péant · L. Eder-Colli
Department of Basic Neuroscience, Medical School, University of Geneva, Geneva, Switzerland

A. Dosso · F. Chiodini (✉)
Laboratory of Cell Biology, Ophthalmology Clinic, Geneva University Hospital, Rue Alcide Jentzer 22, 1211 Geneva 14, Switzerland
e-mail: Florence.Chiodini@hcuge.ch

## Introduction

Müller cell (MC) dysfunction precedes photoreceptor abnormalities in some retinopathies such as glaucoma [1], hepatic retinopathy [2] or in certain autosomal recessive retinal pathologies [3–5] and contributes to retinal degeneration [6, 7]. Moreover, in experimental diabetes, glial reactivity and altered glial glutamate metabolism in MCs are early pathogenic events that may induce retinal degeneration [8–10].

The NSE-Hu-Bcl-2 transgenic mouse (line 71) over-expresses the human form of Bcl-2 (Hu-Bcl2) under the control of the neuron-specific enolase (NSE) promoter [11]. By exploring the consequence of Hu-Bcl2 over-expression in NSE-Hu-Bcl-2 transgenic (tg) mouse retina, Dubois-Dauphin and colleagues [12] showed that tg retinae undergo early postnatal degeneration and that this degeneration is linked to the prior death of MCs which are the only retinal cells expressing the Hu-Bcl-2 transgene. This MC death leads to secondary photoreceptor cell

death from postnatal day (PN) 21. So far, this NSE-Hu-Bcl-2 mouse model of retina degeneration has been only characterized by immunohistochemical approaches [12]. But, no functional retinal studies have been investigated on this model.

Using electroretinographic (ERG) recordings, we wanted to compare the functional changes taking place in degenerative NSE-Hu-Bcl-2 tg mouse at PN15 and PN20 (i.e. just before wide spread death of photoreceptors) to normal retina of C57/Bl6 mouse of the same littermate. We recorded light-intensity responses of retinal cells in both scotopic and photopic conditions. As reported below, our study confirmed the functional maturation of rods and cones in normal postnatal C57/Bl6 strain and dysfunctions of rod- and cone-mediated responses already at 15 days of age during development in NSE-Hu-Bcl-2 tg mice.

## Material and methods

### Animals

The generation of C57/Bl6 hemizygous transgenic mice over-expressing the human Bcl-2 protein (line 71) under the control of the promoter of NSE has been described previously [11]. Pups were generated by crossing hemizygous NSE-Hu-Bcl-2 transgenic males with C57/Bl6 females to generate control and NSE-Hu-Bcl-2 transgenic pups. Thus, age-matched wild-type (WT) and NSE-Hu-Bcl-2 transgenic animals were from the same litter. The genotype of the mice was analyzed by polymerase chain reaction (PCR) from genomic DNA extracted from mouse tail [11]. Mice were kept in an artificial 12 h–12 h light–dark cycle, with an illumination level of 60 phototopic lux. All experimental procedures were carried out in accordance with Federal Swiss Veterinary Regulations and in compliance with the Association for Research in Vision and Ophthalmology (ARVO) statement for the use of animals in Ophthalmic and Vision Research.

### Histology

After sacrifice, eyes were enucleated from wild-type and transgenic mice at PN15 and PN20. Eyecups were dissected out and immediately fixed by one night incubation in 4% paraformaldehyde in PBS (pH 7.4) at 4°C. Tissue was then rinsed extensively in PBS, dehydrated in increasing graded alcohols (70, 90, 95 and 100%) and processed for paraffin embedding. Five μm-thick sections were collected on Superfrost slides (Menzler-Gläser, Braunschweig, Germany). They were then deparaffinized in Neoclear (Merck, Darmstadt, Germany) and rehydrated in decreasing graded alcohols. Sections were stained with haematoxylin-eosin solution and viewed on the Zeiss Axioskop 2 plus microscope. Images were digitalized with an Axiocam camera.

### Electrophysiology

A total of 13 NSE-Hu-Bcl-2 and 19 WT mice, aged of 15 and 20 days, were tested. Mice maintained on a light–dark cycle (12 h–12 h) were dark-adapted overnight (at least 6 h) before experiments. Under dim red light, anaesthesia was induced by intraperitoneal injection of a saline solution containing a mixture of ketamine (Ketalar, 50 mg/kg) and xylazin (Rompun, 25 mg/kg). Their pupils were dilated with a mix of tropicamide (Midriaticum Stulln; Pharm Stulln, Nabburg, Germany) and phenylephrine (Neosynephrin-POS 5%, Ursapharm, Saarbruecken, Germany). The anaesthetized mice were placed in the Ganzfeld bowl on a sliding table. A heating pad allowed maintaining the mouse body temperature at 38°C. Silver needle electrodes served as reference (forehead) and ground (tail) while gold wire rings were used as active electrodes. The ophthalmic methylcellulose solution (Methocel, Ciba Vision, Switzerland) was applied to ensure electrical conductance and to keep the cornea hydrated during the experimental session. The recording set-up featured a Ganzfeld bowl, a DC amplifier, and a computer for stimulus generation and data analysis (RetiPort, Roland Consult, Germany). ERGs were recorded from both eyes simultaneously. Band-pass filter width was set at 1–300 Hz for single flash and flicker stimuli recordings. Single-flashes were obtained both under dark-adapted and light-adapted conditions. Scotopic session started after an overnight dark-adaptation with single flash recordings at light intensities increasing from $10^{-4}$ to 25 candelas*second/$m^2$ (cds/$m^2$), divided into ten steps of 0.5 and

1 log cds/m$^2$. About 30 responses were averaged for stimuli of 0.1, 1, 10, 30, 100, 300 mcds/m$^2$ (inter-stimulus intervals of 5 s) and 15 responses for stimuli of 1, 3, 10, 25 cds/m$^2$ (inter-stimulus intervals of 20 s). Light-adaptation was performed using a steady rod-desensitizing adapting background of 25 cd/m$^2$ applied for 15 min to reach a stable level of the photopic responses. Conditions were same as above but higher frequencies were used: 0.01, 0.1, 0.3, 1, 3, 10, and 25 cds/m$^2$. Photopic flicker stimuli had an intensity of 3 cds/m$^2$ at frequencies from 1 to 30 Hz.

Electroretinographic a- and b-waves were measured in their amplitude (baseline to negative a-wave peak, a-wave to positive b-wave peak, respectively) and time-to-peak (from stimulus onset to negative a-wave or positive b-wave peak, respectively). The results were averaged, and comparisons were made among averaged values across animals. Errors are presented as ±SEM. To analyze the relationship between b-wave amplitude and flash intensity, we used the saturating hyperbolic function Naka–Rushton with the form: $b = (b_{\max,\text{scot}} * I)/(b_{\max,\text{scot}} + I_{0.5})$, where $b_{\max,\text{scot}}$ is the saturated scotopic b-wave amplitude and $I_{0.5}$ is the intensity that provides half saturation. The baseline and peak of each filtered trace were measured, and the data for increasing intensities were fitted to the above equation.

## Results

We analysed ERG parameters in developing C57/Bl6 mice at PN15 and PN20 to assess retinal maturation to compare it to functional changes during degeneration in NSE-Hu-Bcl-2 transgenic mice at the same time points. First, histological sections performed at PN15 and PN20 highlighted a disorganization of the outer nuclear layer (ONL) showing rosettes formed by photoreceptor cell bodies and disappearance of a clearly delimited OPL (Fig. 1B and D). This observation was in accordance with the results previously described by Dubois-Dauphin and colleagues [12].

As retinal degeneration proceeds too fast in this model, no ERG recordings have been realized at time points above PN20. ERG recordings at PN15 and PN20 comprised a range of increasing stimulus intensities in scotopic condition as well as in light-adapted ERGs for pure cone-driven responses. In control mice, in Fig. 2A, typical scotopic responses

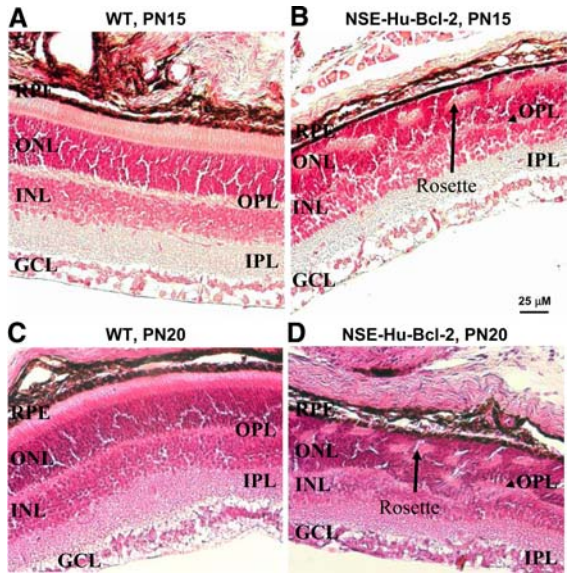


**Fig. 1** Histological views of wild-type (WT) and NSE-Hu-Bcl-2 transgenic retinae from PN15 (**A** and **B**) and PN20 (**C** and **D**) mice. Note the formation of rosettes in the photoreceptor layer in transgenic retina. GCL: Ganglion Cells Layer, IPL: Inner Plexiform Layer, INL: Inner Nuclear Layer, OPL: Outer Plexiform Layer, ONL: Outer Nuclear Layer, RPE: Retinal pigmented epithelium

to a range of stimulus intensity at PN15 and PN20 are depicted, revealing increase in a- and b-waves signal size, decrease in their peak times, and development of marked oscillatory potentials (OPs). The positive b-wave reflects activity of rod-depolarizing bipolar cells [13–15], the negative a-wave activity of almost exclusively rod photoreceptors in the mouse [13–15] and, the OPs,—i.e., wavelets superimposed on the b-wave—reflect interactions among bipolar, amacrine, and ganglion cells [16]. Figure 2B shows on an expanded time scale the a-waves of a family of ERG responses. The averaged stimulus-response functions for a- and b-waves are plotted in Fig. 3A and B, and the typical decrease in implicit time (IT) of the b-wave with retinal maturation is shown in the Fig. 3C. Like for the b-wave, by increasing stimulus intensities and/or as a function of age, a-wave amplitudes increased, while IT decreased, reflecting functional maturation of the retina at PN15 and PN20. The relationship between scotopic b-wave amplitude and intensity can be modelled using a hyperbolic saturation function (see Materials and Methods). In PN15 and PN20 WT mice, the $b_{\max,\text{scot}}$ values measured 150 and 228.6 µV with the $I_{0.5}$

equals to 1.27 and 1.91 scotopic cds/m$^2$, respectively (Fig. 3D). Cone-driven responses recorded in light-adaptation for single flashes as well as for flicker stimulation are shown in Figs. 4 and 5, respectively. As expected, during development and throughout the intensity range examined, the cone ERG increased in amplitude, decreased in IT and developed OPs, reflecting progressive cell maturation and establishment of synaptic connections between cones and other retinal neurons (Fig. 4A). The averaged stimulus-response functions are plotted in Fig. 4B, and the typical decrease of the b-wave IT is shown in the graph of Fig. 4C. Photopic flicker responses were already detected at PN15, but they were weaker than those measured in PN20 eyes at corresponding frequencies (Fig. 5A). By increasing frequencies, the amplitude decreased and reached distinct regular rhythm at 15 Hz in PN15 and PN20 (Fig. 5B), suggesting that photoreceptors are already able to adjust their sensitivity to frequency changes early during postnatal life. Data at PN30 have not been performed but have been already described [17, 18]. In good agreement with previous studies dealing with functional development of retina [13, 14, 19], we showed here at PN15 and PN20 both normal maturation processes in photoreceptors and other retinal neurons in WT postnatal C57/Bl6 mice.

By contrast, in NSE-Hu-Bcl-2 mice, scotopic responses rapidly decreased at PN15 and PN20 leading to profound changes in ERG waveforms of the rod signal (Fig. 2A and B). Note that the graphical overlay of the a-wave responses showed severe decrease until quite disappearance of the rod a-wave signal at PN15 and PN20 (Fig. 2B). When intensity-response function curves were compared with those of control mice, a strong decrease of about 65% of the signal in the rod ERG b-wave amplitudes was already obvious at PN15 (Fig. 3A and B). A steady state of the degeneration between PN15 and PN20 rods activity is observed (Fig. 3B). As shown by the Naka-Rushton equation, and even at highest stimuli, the $b_{max,scot}$ was 56 and 60 μV, respectively for PN15 and PN20 tg mice, the $I_{0.5}$ values being equal to 1.23 and 1.72 scotopic cds/m$^2$ (Fig. 3D). The b-wave IT values expressed as a function of light-intensity at each age were longer in tg mice compared to WT mice (Fig. 3C). Like for scotopic responses, photopic b-wave amplitudes showed a mean decrease of 60% at PN15 (Fig. 4A and B),

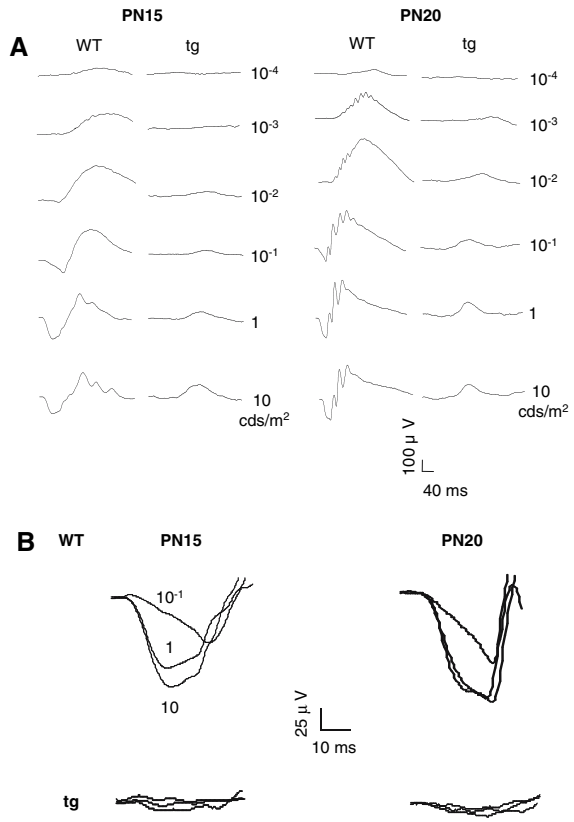


**Fig. 2** Dark-adapted ERG series recorded from wild-type (WT) and from NSE-Hu-Bcl-2 transgenic mice. Representative waveforms averaged from one mouse. Note the calibration for overall smaller amplitude in NSE-Hu-Bcl-2 (tg) compared to WT mice (**A**). Close-up of multiple a-wave responses to flashes of varying intensities from $10^{-1}$ to 10 cds/m$^2$ for WT and tg mice (**B**). Note that the a-wave responses for the tg retinae are overlapped

while IT became longer indicating that cones activity was also affected by retinal degeneration at this stage of maturation (Fig. 4C). A steady state of the degeneration of cones was maintained between PN15 and PN20 (Fig. 4B). Moreover, already at PN15, NSE-Hu-Bcl-2 mice were no longer able to respond to flicker stimuli above 5 Hz. And, by increasing temporal frequency, flicker responses underwent substantial waveform changes, being delayed and expanded in comparison to those observed in WT, reflecting profound alterations in inner nuclear network driven by cones (Fig. 5).

## Discussion

Taken together, our electrophysiological and histological data showed that in NSE-Hu-Bcl-2 tg mice

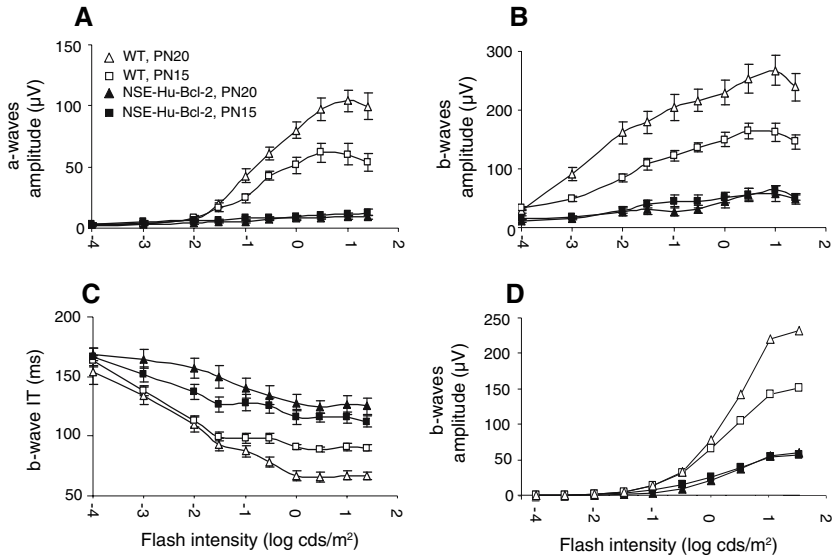


**Fig. 3** Quantification of age-related changes for scotopic a- and b- waves amplitudes (**A** and **B**, white lines, WT; black lines, NSE-Hu-Bcl-2) and IT (**C**, white lines, WT; black bars, NSE-Hu-Bcl-2). B-wave amplitudes, normalized to maximum, as a function of light intensity, fitted by the Naka-Rushton relationship (see Methods) (**D**). Each point represents the average (±SEM) response from 6 to 12 WT mice and from 7 to 8 transgenic mice

development of both rods and cones are markedly affected at the early stage due to MC degeneration. First, histological data coincided with profound and fast structural retinal modifications reported by Dubois-Dauphin and colleagues [12]. They showed formation of hemispherical bundles, i.e. rosettes, of photoreceptors in the ONL starting at PN7, i.e. after the beginning of MC death, and then, massive photoreceptor cell death at PN21. In addition, before any disorganisation of the retina, an important cell death in the INL precedes the period of naturally occurring cell death, leading us to conclude that degeneration is an early event in tg retina probably interfering with retina development. Secondly, at PN15 and PN20 days of age, there was a severe reduction in both scotopic b-waves and rod a-waves, arising from the rods pathway defect after MCs death. This leads to the decreased input to the bipolar cell attributable to the secondary loss of photoreceptors. The cone pathway also degenerated in NSE-Hu-Bcl-2 mice with the cone-driven ERGs reduced to 60% at PN15. Thus, observed ERG responsiveness at PN15 and PN20 should be explained by secondary disruption in photoreceptor morphology in NSE-Hu-Bcl-2 tg model. MC dysfunction or degeneration induces impairment of photoreceptor cell development [7; for review, see 20]. For example, the zebra fish mutant carrying the homozygous recessive mutation *lazy eyes* (*lze*) shows a retina degeneration also induced by a prior MC disruption [20]. This study revealed that mutant ERG recordings had severely reduced a- and b-wave amplitudes relative to wild-type fish, indicating outer retinal dysfunction and furthermore that MC disruption induced secondary changes in photoreceptor differentiation and maturation.

A residual ERG persisted at PN20 although photoreceptor layer of tg retina was profoundly disordered. This may be explained by two small areas escaping retina degeneration, i.e. the peripapillary and extreme peripheral regions [12]. In these regions, MCs do not express the Hu-Bcl-2 transgene and do not degenerate, and both retina cells and retina structure are preserved. In a previous work, Peachey and colleagues [21] showed that Bcl-2 expression, targeted to photoreceptors, induced their cell death but also bipolar cell degeneration. They assumed that Bcl-2 may be released from photoreceptors in the extracellular space and then may affect bipolar cells in a yet undetermined way. We have not yet analyzed bipolar or other retinal cell markers to assess the effect of a potential release of Hu-Bcl-2 by MCs. However, we cannot exclude this phenomenon. Whatever it is, levels of rhodopsin quantified by Western blotting (unpublished data) in the tg retinae were already reduced by 38% at PN10, whereas massive death of photoreceptors was reported to occur only from PN21 onwards [12]. The cause of such an early alteration of rhodopsin level is not clear yet. As over-expression of Hu-Bcl-2 was associated with a reduction in rhodopsin content [22], it might be supposed that rhodopsin down-expression in transgenic mouse retina could result from Hu-Bcl-2

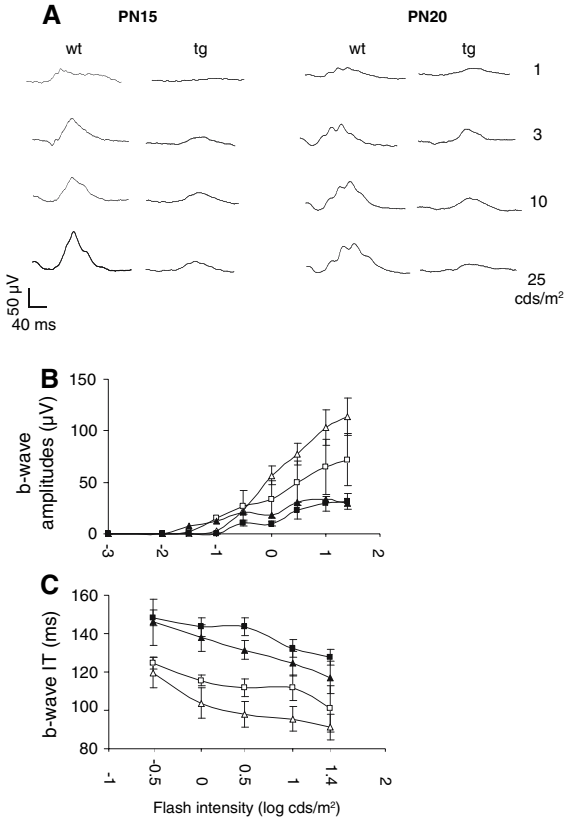


**Fig. 4** Light-adapted single-flash ERG series recorded from wild-type (WT) and from NSE-Hu-Bcl-2 transgenic mice (tg). (**A**) Cone-mediated ERGs recorded at different stimulus intensities from one animal. Traces are averaged. Intensity-response functions for the cone ERG b-wave amplitude (**B**, white lines, WT; black lines, NSE-Hu-Bcl-2) and IT (**C**, white lines, WT; black lines, NSE-Hu-Bcl-2)

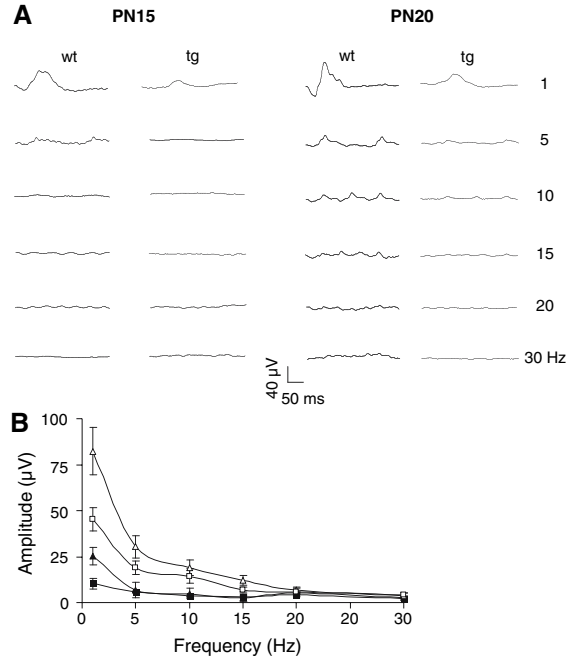


**Fig. 5** Photopic flicker responses. (**A**) Flicker responses to stimuli of varying frequencies (1–30 Hz) but at constant intensity (3 cds/m$^2$) recorded from WT and tg retinas. (**B**) Intensity response functions for flicker ERG. Each point represents the average (±SEM) response from 4 to 8 WT (white lines) mice and from 3 to 5 tg mice (black lines)

release from MCs. But, as rhodopsin was not detectable by immunoblotting at PN5 in both WT and tg mice, we were not able to know if the rhodopsin decrease in the transgenic retina was occurring before MC cell death. Finally, in the mouse line 73, which also over-expresses the Hu-Bcl-2 protein under the control of the NSE promoter, the transgene is overexpressed in all retinal neurons except photoreceptors [11, 23]. This over-expression, described as being protective against naturally occurring cell death (except cholinergic amacrines), does not disturb retina morphology neither does it induce cell death [11, 23, 24]. In this transgenic line, the Hu-Bcl-2 was also ectopically expressed in MCs but there was no apparent effect of the transgene over-expression on MC morphology at least up to 3–4 months of age [23]. Furthermore, ERGs performed on these tg mice up to 11-month-old were similar to those obtained on WT mice [25, 26]. Thus, expression of Hu-Bcl-2 transgene in MCs cells of this mouse strain did not induce MC death either retinal degeneration suggesting that Bcl2 over-expression is not per se deleterious. Then, in our mouse model (line 71), we could not exclude that MC death might reflect an insertional mutation. Indeed, it might be possible that insertion of the transgene has knocked down a gene encoding a protein that is essential for MC survival and/or maturation.

The present work is a functional study complementary to histological study performed by Dubois-Dauphin and colleagues [12]. Further electrophysiological and molecular biology experiments should allow us to better understand mechanisms of NSE activation in MCs of Hu-Bcl2 tg mice and how Hu-Bcl-2 over-expression disrupts the functional and structural integrity of visual cells and lead ultimately to a widespread retinal degeneration.

**Aknowledgements** This work was supported by the Provisu Foundation, Schmidheiny Foundation, De Reuter Foundation and Novartis Foundation grants to L.E-C.

## References

1. Kawasaki A, Otori Y, Barnstable CJ (2000) Müller cell protection of rat retinal ganglion cells from glutamate and nitric oxide neurotoxicity. Invest Ophthalmol Vis Sci 41:3444–3450
2. Reichenbach A, Fuchs U, Kasper M, el Hifnawi E, Eckstein AK (1995) Hepatic retinopathy: morphological features of retinal glial (Müller) cells accompanying hepatic failure. Acta Neuropathol (Berl) 90:273–281
3. Maw MA, Kennedy B, Knight A, Bridges R, Roth KE, Mani EJ, Mukkadan JK, Nancarrow D, Crabb JW, Denton MJ (1997) Mutation of the gene encoding cellular retinaldehyde-binding protein in autosomal recessive retinitis pigmentosa. Nat Genet 17:198–200
4. Morimura H, Berson EL, Dryja TP (1999) Recessive mutations in the RLBP1 gene encoding cellular retinaldehyde-binding protein in a form of retinitis punctata albescens. Invest Ophthalmol Vis Sci 40:1000–1004
5. Saari JC, Crabb JW (2005) Focus on molecules: cellular retinaldehyde-binding protein (CRALBP). Exp Eye Res 81:245–246
6. Bringmann A, Reichenbach A (2001) Role of Müller cells in retinal degenerations. Front Biosci 6:E72–E92
7. Bringmann A, Pannicke T, Grosche J, Francke M, Wiedemann P, Skatchkov SN, Osborne NN, Reichenbach A (2006) Müller cells in the healthy and diseased retina. Prog Retin Eye Res 25:397–424
8. Li Q, Puro DG (2002) Diabetes-induced dysfunction of the glutamate transporter in retinal Müller cells. Invest Ophthalmol Vis Sci 43:3109–3116
9. Lieth E, Barber AJ, Xu B, Dice C, Ratz MJ, Tanase D, Strother JM (1998) Glial reactivity and impaired glutamate metabolism in short-term experimental diabetic retinopathy. Penn State Retina Research Group. Diabetes 47: 815–820
10. Rungger-Brändle E, Dosso AA, Leuenberger PM (2000) Glial reactivity, an early feature of diabetic retinopathy. Invest Ophthalmol Vis Sci 41:1971–1980
11. Martinou JC, Dubois-Dauphin M, Staple JK, Rodriguez I, Frankowski H, Missotten M, Albertini P, Talabot D, Catsicas S, Pietra C (1994) Overexpression of BCL-2 in transgenic mice protects neurons from naturally occurring cell death and experimental ischemia. Neuron 13: 1017–1030
12. Dubois-Dauphin M, Poitry-Yamate C, de Bilbao F, Julliard AK, Jourdan F, Donati G (2000) Early postnatal Müller cell death leads to retinal but not optic nerve degeneration in NSE-Hu-Bcl-2 transgenic mice. Neuroscience 95:9–21
13. Bonaventure N, Karli P (1968) Maturation of ERG and evoked visual potentials in mice. C R Seances Soc Biol Fil 162:553–555
14. el Azazi M, Wachtmeister L (1990) The postnatal development of the oscillatory potentials of the electroretinogram. I. Basic characteristics. Acta Ophthalmol (Copenh) 68: 401–409
15. Lyubarsky AL, Pugh EN Jr (1996) Recovery phase of the murine rod photoresponse reconstructed from electroretinographic recordings. J Neurosci 16:563–571
16. Wachtmeister L (1998) Oscillatory potentials in the retina: what do they reveal. Prog Retin Eye Res 17:485–521
17. Jaissle GB, May CA, Reinhard J, Kohler K, Fauser S, Lutjen-Drecoll E, Zrenner E, Seeliger MW (2001) Evaluation of the rhodopsin knockout mouse as a model of pure cone function. Invest Ophthalmol Vis Sci 42:506–513
18. Peachey NS, Goto Y, al Ubaidi MR, Naash MI (1993) Properties of the mouse cone-mediated electroretinogram during light adaptation. Neurosci Lett 162:9–11
19. Fulton AB, Hansen RM, Findl O (1995) The development of the rod photoresponse from dark-adapted rats. Invest Ophthalmol Vis Sci 36:1038–1045
20. Kainz PM, Adolph AR, Wong KY, Dowling JE (2003) Lazy eyes zebrafish mutation affects Müller glial cells, compromising photoreceptor function and causing partial blindness. J Comp Neurol 463:265–280
21. Peachey NS, Quiambao AB, Xu X, Pardue MT, Roveri L, McCall MA, al Ubaidi MR (2003) Loss of bipolar cells resulting from the expression of bcl-2 directed by the IRBP promoter. Exp Eye Res 77:477–483
22. Joseph RM, Li T (1996) Overexpression of Bcl-2 or Bcl-XL transgenes and photoreceptor degeneration. Invest Ophthalmol Vis Sci 37:2434–2446
23. Strettoi E, Volpini M (2002) Retinal organization in the bcl-2-overexpressing transgenic mouse. J Comp Neurol 446:1–10
24. Cenni MC, Bonfanti L, Martinou JC, Ratto GM, Strettoi E, Maffei L (1996) Long-term survival of retinal ganglion cells following optic nerve section in adult bcl-2 transgenic mice. Eur J Neurosci 8:1735–1745
25. Gianfranceschi L, Fiorentini A, Maffei L (1999) Behavioural visual acuity of wild type and bcl2 transgenic mouse. Vision Res 39:569–574
26. Porciatti V, Pizzorusso T, Cenni MC, Maffei L (1996) The visual response of retinal ganglion cells is not altered by optic nerve transection in transgenic mice overexpressing Bcl-2. Proc Natl Acad Sci U S A 93:14955–14959